Investigation of the Concentration- and Temperature-Dependent Motion of Colloidal Nanoparticles

Barnaby Handel,[a] Vladislava Vladimirova,[a] Erving Ximendes,[a,b] José García Solé,[a] Daniel Jaque,[a,b]* Riccardo Marin[a]*

[a] Fluorescence Imaging Group (FIG), Departamento de Física de Materiales, Facultad de Ciencias, Universidad Autónoma de Madrid, C/ Francisco Tomás y Valiente 7, Madrid 28049, Spain.

[b] Nanobiology Group, Instituto Ramón y Cajal de Investigación, Sanitaria Hospital Ramón y Cajal, Ctra. De Colmenar Viejo, Km. 9100, 28034 Madrid, Spain

Table of Contents

Experimental details.

The PEGylated gold nanoshells (GNSs) were purchased from NanoComposix (San Diego, CA).

Optical extinction spectra were recorded at room temperature with an UV/VIS/NIR spectrophotometer (Perkin Elmer Lambda1050, Waltham, MA).

For the laser speckle analysis, a moorFLPI-2 Full-Field Laser Perfusion Imager (Millwey, Devon, UK) equipped with a (785 ± 10) nm near-infrared semiconductor diode laser of 0.4 mW maximum accessible power was used. Backscattered laser light was collected and integrated by a CCD camera to produce a contrast image. The imager was connected to a computer running the moorFLPI-2 Measurement software, which produces a map of laser-speckle contrast analysis (LASCA) intensity.

Spatial processing was preferred over temporal processing. This processing method compares the variation between 5x5 blocks of pixels (kernel) to build a contrast image. The standardized integration time of the camera for the instrument is 20 ms. A frame rate of 5 Hz was used and.

For experiments under an imposed flow, a plastic tubing with an internal and external diameter of 5 and 3 mm respectively was used. Volumetric flow was imposed using a New Era NE-1002X Microfluidics Syringe Pump (Toledo, NY). Ten-mL syringes were used, which allowed a maximum flow rate of 367 mL min^{-1}, with a resolution of 0.1 mL min^{-1}. Typically, 1 or 2-minute videos were recorded and several frames extracted from them. Before each measurement, the nanoparticle suspension was sonicated in an ultrasonic bath for at least 1 min. The intensity was calculated for each frame integrating the signal in the image over a region of interest (ROI) that did not encompass the wall of the tubing. The ROI was kept constant throughout each series of measurements with a specific nanofluid concentration.

For temperature-dependent measurements, a square-section (0.5-mm edge) glass microchamber was put in contact with a heating stage and heating-cooling cycles were performed in the 20-60 °C range at a continuous rate of 1 °C min^{-1}. For each frame, the intensity was calculated for each frame integrating the signal over a ROI, whose position was kept constant for all the images obtained from this experiment.

Uncertainties.

The random error on speckle flux readings was estimated from the statistic analysis performed on >100 LASCA frames obtained from the LASCA videos recorded with MOORFLPI-2 system.

An uncertainty of 0.1 mm was assigned to the measurement of the radius of the tubing, as this was the resolution of the caliper used to take the reading. Similarly, volumetric flux readings

were assigned uncertainties of 0.1 mL min^{-1}, given that this was the resolution of the syringe pump display. The radius and volumetric flux uncertainties were combined using standard error propagation to get fluid velocity uncertainties.

LASCA intensity and observed velocity.

According to LASCA general theory, and as reported in the main text, the speckle contrast K is obtained from the ratio between the standard deviation σ and the average intensity I evaluated, in the case of spatial contrast, over a kernel (*i.e.*, a group) of pixels.[1]

$$K = \frac{\sigma}{I} \qquad (S1)$$

Although theoretically the contrast might vary between 0 and 1, in practice it never exceeds 0.5. Because of this, the above equation can be rewritten as:

$$K = \sqrt{\frac{\tau_C}{2t}} \qquad (S2)$$

Where t is the camera integration time and τ_C is the correlation time. This latter parameter is equal to:

$$\tau_C = \frac{1}{\alpha \cdot k_0 \cdot v} \qquad (S3)$$

Where α is an arbitrary factor that accounts for the Lorentzian width of the scattered spectrum and the optical properties of the medium, k_0 is the wavenumber of the probing light and v is the average velocity of the particles. The instrument used for this study returns a LASCA image of the observed system, where the intensity (I_{LASCA}) is proportional to the flux of the liquid (often referred to as perfusion, since it is applied for the investigation of blood motion). According to the instrument's manual:[1]

$$Flux\ /\ Perfusion \propto \left(\frac{I}{\sigma}\right)^2 \qquad (S4)$$

This holds true when considering that the perfusion is proportional to the average velocity v. Therefore:
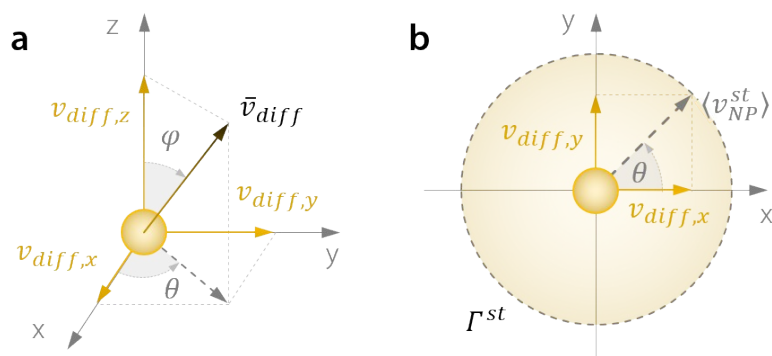
$$I_{LASCA} \propto Flux\ /\ Perfusion \propto v \propto \left(\frac{I}{\sigma}\right)^2 \qquad (S5)$$

Dependence of the speckle intensity on the particle concentration.
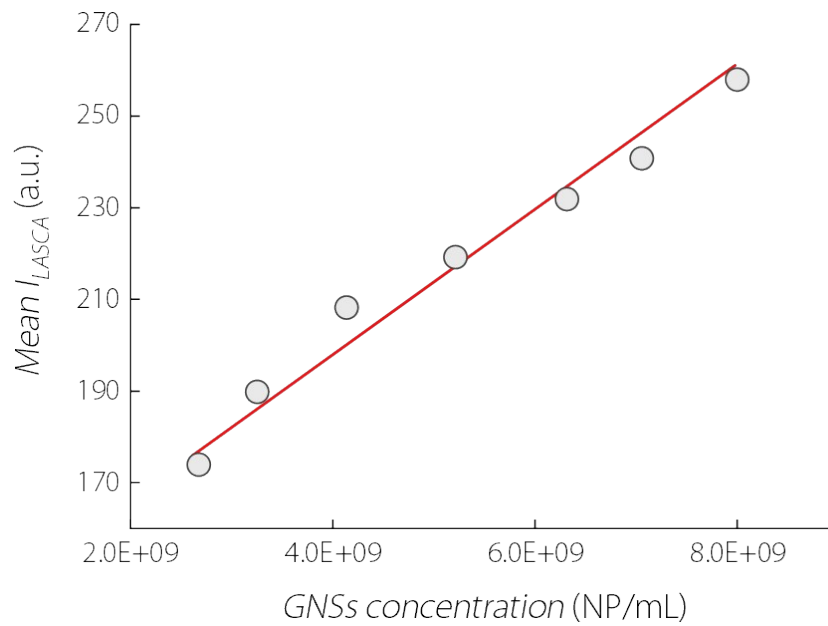
Figure S1. Linear relationship between the nanoparticle concentration and the intensity of the signal recorded by the speckle imaging system used in our study.

Geometrical factors: part I.

Figure S2. a) 3D representation of the diffusion-governed motion of a nanoparticles and **b)** its 2D projection on the *xy* plane.

   With laser speckle imaging, the 3D motion of a nanoparticle is projected on a plane perpendicular to the observation direction. In the static case, the GNS motion is governed exclusively by the random diffusion (**Figure 2a, b**), while with the application of an external flow, results in an additional contribution to the total velocity (**Figure 2c**).

Static conditions.

The apparent velocity of the nanoparticle only depends on the diffusion, and it is determined by the duration of the observation. In our experimental conditions, this is at least equal to the exposure time of the speckle imaging system, *i.e.*, 20 ms. This time is much longer than the characteristic timescales at which the ballistic and hydrodynamic regimes are observable for the system under study. In the case of a 3D system (**Figure 2a**), we can define three axes (*x, y, z*) and two angles (*θ, φ*) such that the apparent velocity of the nanoparticle is:

$$\bar{v}_{NP}^{st} = v_{diff} = v_{diff,x}\hat{x} + v_{diff,y}\hat{y} + v_{diff,z}\hat{z} \tag{S6}$$

Where the components along the three axes are:

$$v_{diff,x} = v_{diff}\sin\varphi\cos\theta \tag{S7}$$

$$v_{diff,y} = v_{diff}\sin\varphi\sin\theta \tag{S8}$$

$$v_{diff,z} = v_{diff}\cos\varphi \tag{S9}$$

When projecting the motion in 2D on the *xy* plane, the magnitude of the velocity is:

$$\left|\bar{v}_{NP}^{st}\right|^{2D} = \sqrt{v_{diff,x}^2 + v_{diff,y}^2} = \sqrt{v_{diff}^2 \sin^2\varphi \cos} \quad \text{(S10)}$$
$$= v_{diff}\sin\varphi$$

So, the magnitude of the velocity projected in 2D only depends on the azimuthal angle φ. Because of this dependence, to retrieve the average value of $\left|\bar{v}_{NP}^{st}\right|^{2D}$ – which equals $\langle v_{NP}^{st}\rangle$ – we can consider the motion of a nanoparticle diffusing in one of the two octants with positive x and z coordinates. The average velocity that is observed projected on the xy plane is hence:

$$\left|\bar{v}_{NP}^{st}\right|^{2D} = \langle v_{NP}^{st}\rangle = \frac{\displaystyle\int_0^{\frac{\pi}{2}} v_{diff}\sin\varphi\, d\varphi}{\displaystyle\int_0^{\frac{\pi}{2}} d\varphi} = \frac{2}{\pi}v_{diff}[-\cos\varphi]_0^{\frac{\pi}{2}} = \frac{2}{\pi}v_{diff} \quad \text{(S11)}$$

This function has no dependence on the angle θ. Therefore, we can visualize this velocity as a vector describing a circumference (Γ^{st}) of radius $\frac{2}{\pi}v_{diff}$ and centred on the nanoparticle (**Figure 2b**).

Geometrical factors: part II.

Because laser-speckle imaging is a technique that affords a 2D projection of 3D objects, geometrical factors are influencing the observed motion of the particles. In the present case, for instance, the probed volume, and hence the number of nanoparticles, is not constant. This is exemplified in **Figure S3**, where a yz section of the tubing containing the GNS nanofluid is shown. Following this observation, we can re-write Equation 3 of the main manuscript of the main manuscript to highlight the presence of a geometrical correction factor:

$$I_{LASCA}^{st}(y) = \beta N \langle v_{NP}^{st} \rangle = \beta' \Omega(y) N \langle v_{NP}^{st} \rangle \tag{S12}$$

Where β' is the correction factor after the separation of the geometrical correction factor (Ω). This latter correction factor is obtained considering the integral area of the circumference having the center on the axis of the tubing and the inner diameter of the tubing (d) for diameter. Considering the positive z semiaxis, the circumference has formula:

$$z(y) = \sqrt{\left(\frac{d}{2}\right)^2 - y^2} \tag{S13}$$

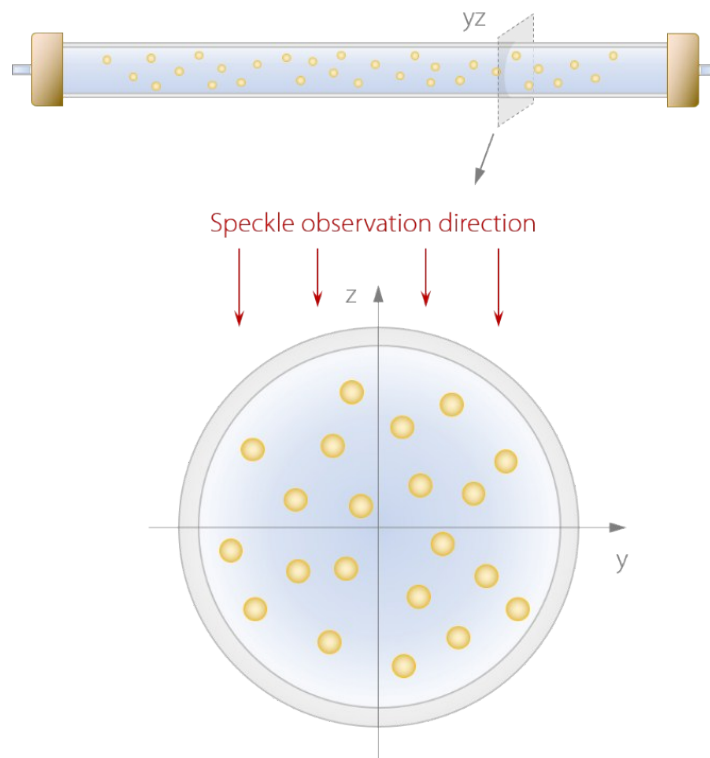The area of the circle delimited by this circumference can be retrieved from the integral:

$$Area = 4 \int_0^{\frac{d}{2}} \sqrt{\left(\frac{d}{2}\right)^2 - y^2} \, dy \tag{S14}$$

This integral has the general formula:

$$\int \sqrt{A^2 - y^2} \, dy = \frac{y}{2}\sqrt{A^2 - y^2} + \frac{A^2}{2} \text{asin}\left(\frac{y}{A}\right) + C \tag{S15}$$

Given the above, the area as a function of y, is given by the following expression:

$$Area(y) = \begin{cases} \frac{d^2}{4}\left(\frac{\pi}{2} + asin\left(\frac{2y}{d}\right)\right) + y\sqrt{\frac{d^2}{4} - y^2}, & -\frac{d}{2} < y < 0 \\ \frac{d^2}{4}\left(\frac{\pi}{2} - asin\left(\frac{2y}{d}\right)\right) - y\sqrt{\frac{d^2}{4} - y^2}, & 0 < y < \frac{d}{2} \end{cases} \tag{S16}$$

Figure S3. Sketch of the tubing used for the experiments under imposed flow and its transverse section.

The geometrical correction factor for the LASCA intensity is therefore obtained by simply multiplying the area by an arbitrary value h, which is the length of the considered tubing portion:

$$Volume(y) = \Omega(y) = \begin{cases} \left[\frac{d^2}{4}\left(\frac{\pi}{2} + asin\left(\frac{2y}{d}\right)\right) + y\sqrt{\frac{d^2}{4} - y^2}\right]h, & -\frac{d}{2} < y < 0 \\ \left[\frac{d^2}{4}\left(\frac{\pi}{2} - asin\left(\frac{2y}{d}\right)\right) - y\sqrt{\frac{d^2}{4} - y^2}\right]h, & 0 < y < \frac{d}{2} \end{cases} \tag{S17}$$

We tested the validity of our assumption upon analyzing the I_{LASCA}^{st} profile of a LASCA image taken for a static colloid (volume fraction, $\Box = 3 \cdot 10^{-4}$ %) at room temperature (**Figure S4**). To obtain the plot in **Figure S4b**, the ROI was considered as composed of w columns of size 1xh pixels. The average intensity and corresponding standard deviation at each x were obtained from the integration of the LASCA signal over each column, analyzing at least 200 frames. The diameter d in pixels (71.5) was obtained from the LASCA image (**Figure S4a**) and the knowledge that the tubing has an external and internal diameter of 5 and 3 mm,
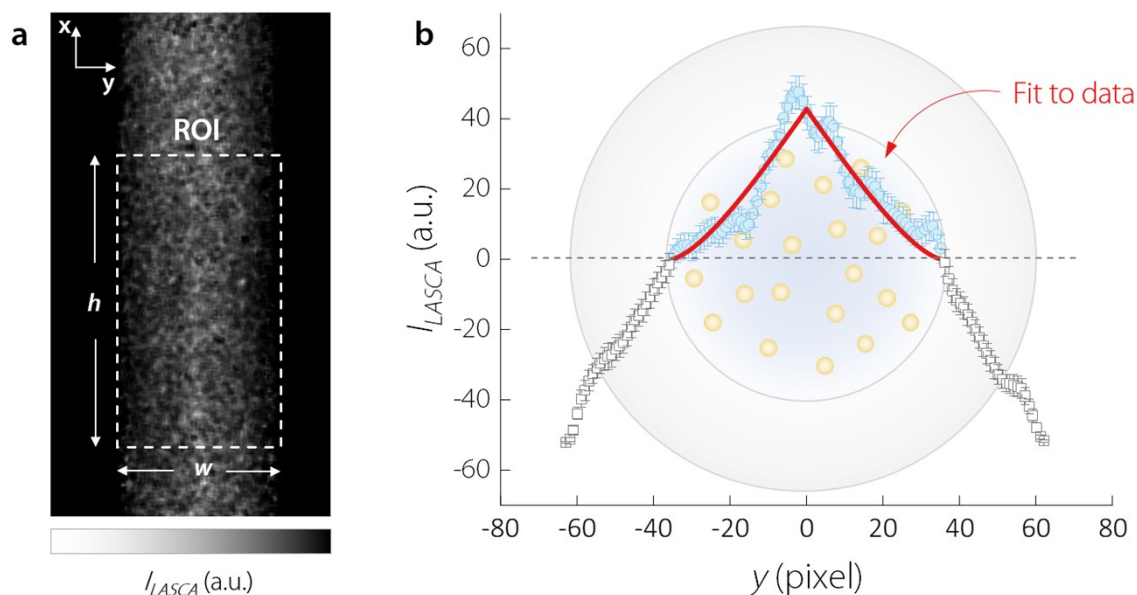
Figure S4. a) representative gray-scale LASCA image taken for a static colloid (volume fraction, $\varPi$ = 3·10^{-4} %) at room temperature inside a tubing. b) Intensity profile plot along the y-axis (gray squares and azure circles) obtained from the analysis of the region of interest (ROI) highlighted in a and its fit according to Equation S18 (red lines).

respectively. This value (d = 71.5 pixel) was kept fixed during the fitting procedure. Before the fitting procedure, the experimental data were shifted in order to have an intensity of 0 at the internal wall of the tubing. Finally, we introduced in Equation S12 a scale factor (b) that factors in the length of the tubing portion considered (h), the rest of the parameters in Equation S12. Therefore, the expression used for the fitting procedure was:

$$I_{LASCA}^{st}(y) = \begin{cases} b\left[\dfrac{d^2}{4}\left(\dfrac{\pi}{2} + asin\left(\dfrac{2y}{d}\right)\right) + y\sqrt{\dfrac{d^2}{4} - y^2}\right], & -\dfrac{d}{2} < y < 0 \\ b\left[\dfrac{d^2}{4}\left(\dfrac{\pi}{2} - asin\left(\dfrac{2y}{d}\right)\right) - y\sqrt{\dfrac{d^2}{4} - y^2}\right], & 0 < y < \dfrac{d}{2} \end{cases} \qquad \text{(S18)}$$
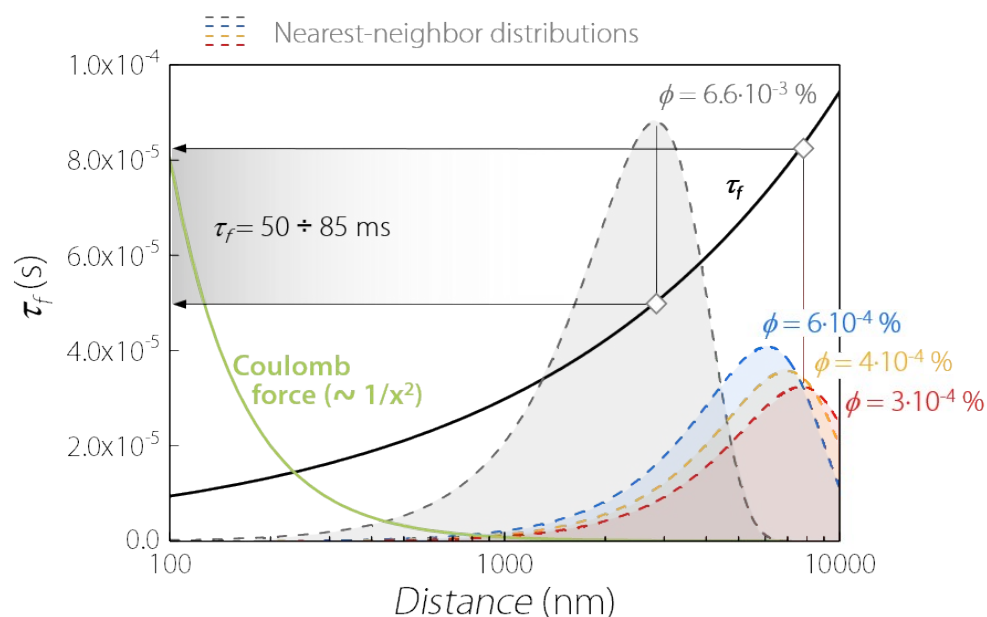
The fit for both negative and positive y values returned compatible values of b: (0.0220 ± 0.0008) and (0.0216 ± 0.0006), respectively. R^2-values were 0.90 and 0.89 for negative and positive y values.

# Selection of the best plasmonic gold nanoshells for laser speckle imaging.
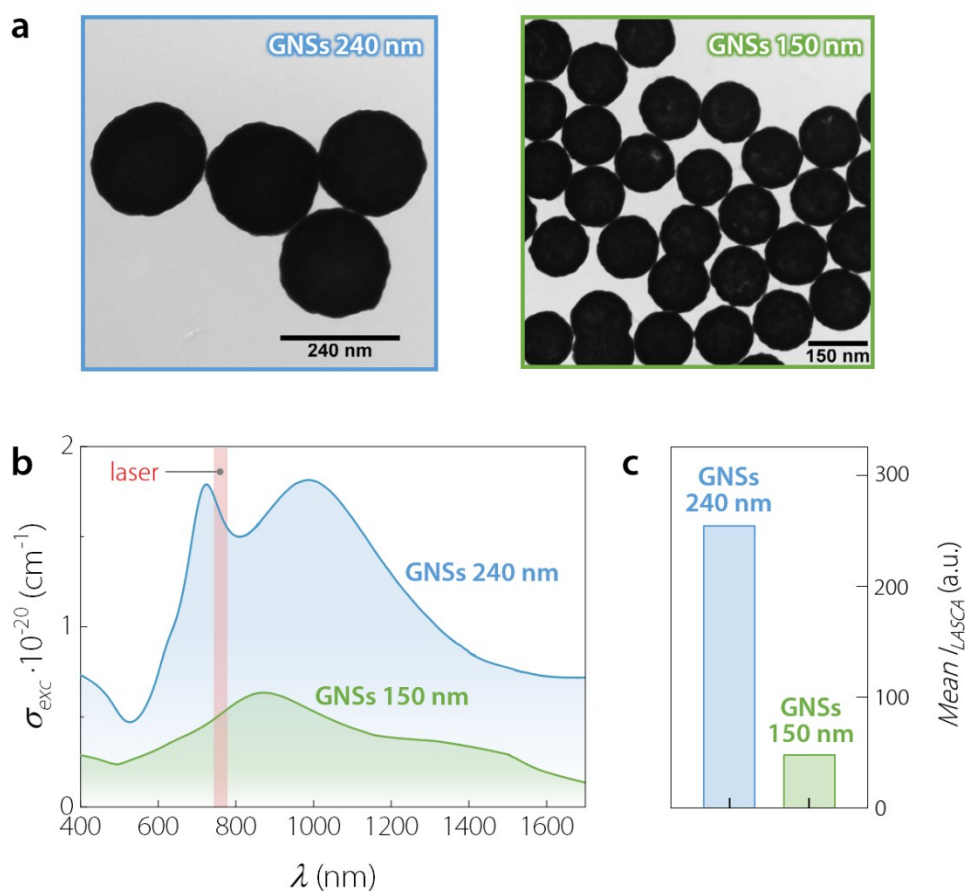
Figure S5. a) representative transmission electron microscopy (TEM) images of two gold nanoshells (GNSs) of different diameters (150 and 240 nm) whose behavior in speckle imaging was tested, along with their b) extinction spectra (the laser speckle wavelength range is also indicated with a red rectangle) and c) a characteristic speckle intensity observed for LASCA images obtained from suspensions of same volume fraction ($f = 6 \cdot 10^{-3}$ %). It is evident how to a larger light extinction cross section corresponds a higher LASCA intensity. Following this observation, 240-nm-diameter GNSs were selected for the study. TEM images are taken from the website of the supplier (NanoComposix, https://nanocomposix.com/collections/all/products/nanoxact-gold-nanoshells-pvp?variant=15906896412761).

Nearest-neighbor distributions and long-range interactions between particles.

Figure S6. Nearest-neighbor probability distributions (dashed curves). Each curve returns the probability of finding the first particle – nearest-neighbor – within a certain distance from the particle chosen as the reference for the four explored GNS concentrations. These curves have been determined considering the GNS concentration and Equation 671 in Reference 2. The solid black line shows the time (τ_f) required for a fluid vorticity (result of the non-laminar flow at the nanoparticle's surface) to travel a specific distance.[3] The time (50-85 µs) required by the fluid to travel a distance of the order of the nearest-neighbor distance is on a short enough timescale to conceivably have a sizeable impact on the motion of the suspended nanoparticles. The solid green line is a simple $1/x^2$ function simulating the trend of a Coulombic force acting between two charged centers of arbitrary surface charge. The overlap with the tail at shorter distances of the nearest-neighbor distributions suggests a possible contribution of this interaction in the Brownian motion of the GNSs at high concentrations.

Temperature-dependence of the scattering cross section.
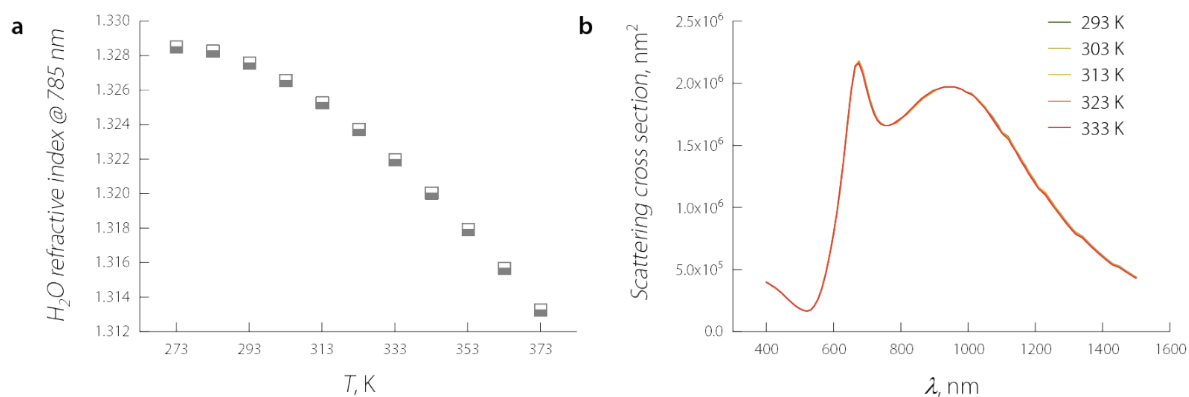
Figure S7. a) Variation of the refractive index of water at 785 nm over the 273-373 K range as obtained from Ref. 4. **b**) Variation of the scattering cross section of the GNSs used in this study over the temperature range employed for the temperature-dependent study (293-333 K). The plots were obtained from the website of the GNSs supplier[5] using the values of refractive index from **a**.

REFERENCES

1. moorFLPI-2 User Manual, **2017**, Moor Instruments Limited, Millwey, Axminster, Devon, EX13 5HU, UK.
2. Chandrasekhar, S. *Reviews of Modern Physics* **1943**, *15*, 1-89.
3. Kheifets, S.; Simha, A.; Melin, K.; Li, T.; Raizen, M. G. *Science* **2014**, *343*, 1493-1496.
4. Bashkatov, A. N.; Genina, E. A. *SPIE Proceedings* **2003** *5068* – DOI: 10.1117/12.518857
5. https://nanocomposix.com/pages/tools#target